RESEARCH ARTICLE

Empowering the Future of Hybrid MIMO-RF UOWC: Advanced Statistical Framework for Channel Modeling and Optimization for the Post-5G Era and Beyond

LATIF JAN[1], (Member, IEEE), **GHASSAN HUSNAIN**[1], **WALEED TARIQ SETHI**[2], **IHTISHAM UL HAQ**[3], **YAZEED YASIN GHADI**[4], AND **HEND KHALID ALKAHTANI**[5]

[1]Department of Computer Science, Iqra National University, Peshawar 25100, Pakistan
[2]Faculty of Electrical Engineering, Ghulam Ishaq Khan Institute of Engineering Sciences and Technology, Topi, Khyber Pakhtunkhwa 23640, Pakistan
[3]Department of Mechatronic Engineering, University of Engineering and Technology, Peshawar, Peshawar 25000, Pakistan
[4]Department of Computer Science and Software Engineering, Al Ain University, Al Ain, United Arab Emirates
[5]Department of Information Systems, College of Computer and Information Sciences, Princess Nourah bint Abdulrahman University, Riyadh 11671, Saudi Arabia

Corresponding authors: Hend Khalid Alkahtani (Hkalqahtani@pnu.edu.sa) and Ghassan Husnain (ghassan.husnain@gmail.com)

ABSTRACT This research work examines the reliability of a wireless communication system that uses a hybrid radio frequency (RF) and underwater optical wireless communication (UOWC) in a dual-hop system. The proposed system consists of a single source (S) node that sends information to a destination (D) node through an amplify-and-forward (AF) relay (R) node using a multiple-input multiple-output (MIMO)-RF and UOWC links. The channel between the (S) node is subject to Nakagami-m fading using a transmit antenna selection (TAS) technique and maximal ratio combining (MRC) at (R) node, and exponential generalized gamma distribution (EGG) at (D) node to evaluate the overall statistical analysis of the proposed end-to-end(E2E) system. The proposed system has been extensively tested and validated under various conditions using a novel cumulative distribution function(CDF) and probability density function(pdf) whereas; the paper provides closed-form expressions for the outage probability (OP) and average bit error rate (BER) for each channel model.

INDEX TERMS Bit error rate, maximal ratio combining, multiple-input multiple-output-radio-frequency, outage probability, transmit antenna selection, underwater optical wireless communication.

I. INTRODUCTION

A. BACKGROUND

The use of underwater optical wireless communication (UOWC), a hybrid technique of communication that combines radio frequency (RF), is becoming more popular.It provides the most expected surprises and several significant technological breakthroughs, especially in terms of spectrum efficiency, positioning it as a potential competitor technology for the mobile phone networks of the future [1].In [2] the significance and efficacy of UOWC's real-time and

The associate editor coordinating the review of this manuscript and approving it for publication was Xuebo Zhang.

high-throughput applications are discussed, while Campagnaro (2016) describes the acoustic counterpart that makes up the communications via acoustic-optical hybrids. Unfortunately, the UOWC system's performance is severely limited by turbulence, absorption, and scattering. Loss of energy and changes in direction occur as photons transit underwater is displayed by scattering and absorption, which have been thoroughly examined in [3]. The UOWC system performs worse under conditions of turbulence because of signal fading caused by the rapid refractive index fluctuation along the optical field's path through the water medium as a result of variations in temperature, pressure, salt levels, and air bubbles. On the other hand, UOWC systems

frequently use both horizontal and vertical connection arrangements. The vertical configuration has not gotten significant attention, except for some coverage in [4] and [5], but the horizontal configuration has been thoroughly explored thus far.

According to [6], UOWC constitutes one of the most promising and emerging phenomena in this period of technology, whereas the most seriously impacted optical features undersea are produced by absorption, scattering, and turbulence. Whilst absorption and scattering are the other major underwater constraints mentioned above, turbulence effects are significant and must not be neglected in this study, as indicated in [7] and [8].

The paper in [7] describes how three basic degradation phenomena—absorption, scattering, and fading—affect optical signal transmission across underwater channels. Research studies were conducted to determine the various factors, such as erratic changes in salinity and temperature and the existence of air bubbles as well. This research aimed to understand the impact of these factors on the strength of the optical signal transmitted through the channel. The study evaluated several statistical distributions to determine the probability model that best fits the experimental data. The variations in the water refractive index were also taken into account as they affect the propagation of the optical signal. Additionally, the channel coherence time was acquired to deal with the average duration of fading temporal fluctuations. Based on how well they fit the experimental data, several statistical distributions are then evaluated for correctness. changes in the refractive index of water are introduced throughout the path of propagation by several situations that are created. To deal with the average duration of fading temporal fluctuations, it additionally acquired the channel coherence time.

Temporal dispersion experiments refer to experiments that measure the time delay between the transmission and reception of a signal. The authors in [9] suggest that conducting these experiments in different water types will provide valuable information about how the system performs in different environments. Geographic dispersion refers to the scattering of light due to atmospheric conditions such as haze, fog, and clouds. Duntley and his colleagues conducted experiments to study the effects of geographic dispersion on light transmission. Overall, the authors suggest that conducting experiments in different types of water will provide valuable information about the performance of the wireless communication system in different environments.

The spatial dispersion of photons caused by scattering presents a significant obstacle to the implementation of optical networks underwater. The optical beam's spatial dispersion lowers the photon density at the receiver point. As a result, optical connections are only anticipated to be most useful in lengths under 100m. However, it seems that end users could be willing to put up with a short link range in exchange for the potential increase in information capacity that optical lines could offer. Further research is being done on the effects of spatial spreading on the time-encoded part of the transmitted optical signal. Inter-symbol interference (ISI), which can be brought on by temporal dispersion brought on by several scattering events, can further restrict connection range and/or capacity in [10].

Numerous theoretical models have been developed to forecast the attenuation of signals and capacity for underwater optical connections as a result of the increasing demand for underwater optical connectivity. Because quantifying temporal dispersion in such demanding conditions is difficult, experimental validation of these models is sparse at best. By contrasting the mathematical Monte Carlo (MC) model with actual data, this effort aims to bridge the gap between research and theory. In [11], the authors measure the attenuation and frequency response of a channel with a line-of-sight configuration over a range of 20 attenuation lengths, all the way out to 1 GHz. In [12], a MC numerical simulation is discussed and validated to determine the received power of an optical communication system submerged in water. Power loss is modeled between the transmitter and receiver for several different aperture sizes and FOVs.

In the work cited in [13], the exponentially lognormal and the increasing exponential generalized gamma are further fading types that are taken into consideration. To choose the ideal biassed distribution, the cross-entropy optimization approach is applied. Based on simulations, the importance sampling estimator can achieve the same level of reliability as a naive MC with a far smaller sample size.

Pressure, temperature, and also most especially tidal currents may all have a sudden impact on it as discussed in [14]. Comparable to the way the examination of the impact of saline water is assessed in [15] and [16], the modulation strategies of a UOWC as being similarly relevant for inclusion in this work.

In contrast, [17] points out that the widespread use of multiple antennas, also known as MIMO in wireless relay networks, has indeed been acknowledged as still being crucial in combating the rise in transmission reliability and channel fading tactics. Key research and their application in the usage of the AF relaying technique are thought to be advantageous for multiple antennas, and therefore, it is explored in [18] how it might enable beam-forming methods. Additionally in [19], it points out that the constant system design problem of increasing the number of antennas on both ends makes the deployment of the system highly complicated. Furthermore, the signal generated by MIMO communication systems grows exponentially with the number of antennas, according to [20]. It manages the variety of the broadcast and receivers, which is inspired by an efficient antenna selection approach being more beneficial to enhance the computational overhead. Moreover, antenna selection minimizes the sophistication of signal processing and associated feedback overhead.

To determine the most accurate estimates of the model parameters lambda, w, x, y, and z, we employ the expectation maximization (EM) method. Starting with a set of chosen initial values for the parameters, the EM method iteratively refines the model until convergence is achieved. Thus, the EM technique offers the variables that result in the best fit between the proposed model and the data being analyzed. These numbers shift depending on the temperature, salinity, and number of air bubbles in the water, as shown in Table 1 and Table 2.

B. LITERATURE WORK

The research community in academia has shown a keen interest in the development of underwater optical wireless communication (UOWC) technology. This interest has been demonstrated through various research investigations, such as those cited in [21]. UOWC is seen as a potential quality of both radio frequency (RF) and underwater technologies, particularly since 2020 as cited in [22]. Deep ocean techniques, including UOWC, are expected to become increasingly important in the 21st century due to their significance in a wide range of applications, such as surveillance systems, oil drilling and processing, environmental monitoring, and climate-related operations [23]. Existing RF and acoustic technologies have limitations in terms of restricted and inadequate bandwidth, as noted. Therefore, UOWC is considered to be a more effective high-speed sub-sea communication technology, with the potential to provide enhanced data rates of tens of gigabits per second (Gbps) at 10 meters as stated in [24]. UOWC is also praised for its low latency, high efficiency, and strong inherent security, making it a viable alternative to acoustics in the undersea medium. Laser-induced fluctuations have been used to assess the probabilistic properties of light temperature-based turbulence in UOWC systems, which has drawn a lot of interest in the literature, as mentioned. The highlighted text discusses the limitations of acoustic undersea communication systems, which encounter temporal delays in their communication systems due to scattering, absorbance, and turbulent variations. Real-time performance is still a challenge for networks of communication using an auditory medium, as described in [25]. In contrast, the UOWC technique has been given more attention in recent works due to its potential for high-speed communications and increased capacity. Accordingly, using UOWC surpasses acoustic communication. UOWC has also been praised for its low latency, high efficiency, and strong inherent security, making it a viable alternative to acoustics in the undersea medium. The technique of using laser-induced fluctuations to assess the probabilistic properties of light temperature-based turbulence in UOWC systems has drawn much interest in the literature, as mentioned in [26]. A hybrid triple hop terrestrial free-space optical (FSO), fibre optic cable (FOC), and underwater optical wireless communication (UOWC) link for supplying high-speed optical connectivity between onshore and submerged systems are investigated in detail in the article [27]. The transmission rate and dependability of the UOWC connection are significantly decreased by UOWC, scattering, absorption, and turbulence. While in [28], a downlink non-orthogonal multiple access (NOMA) enabled dual-hop hybrid RF-UOWC with decode and forward (DF) relaying are studied. The RF channel is characterized by Rayleigh fading, while the UOWC channels are characterized by exponential-generalized Gamma (EGG) fading.

The proposal made by an author in [29] regarding the use of the generalized Gamma (gG) distribution as an accurate model for underwater optical wireless communication (UOWC) channels that have temperature gradients. This proposal is significant because it helps in understanding the behavior of UOWC channels in different temperature conditions, which is crucial for designing effective communication systems. The gG distribution is a statistical model used to describe a random variable's probability distribution. It is a generalization of the Gamma distribution and can be used to model a wide range of phenomena. The use of the gG distribution in modeling UOWC channels with temperature gradients is based on the fact that the distribution can capture the effects of both fading and shadowing, which are common in UOWC channels. The study was conducted in [30] to assess the effectiveness of the system's confidentiality in a two-hop hybrid RF-UOWC system. In this study, the authors modeled the decode-and-forward(DF) relay using two different statistical distributions, namely the alpha-mu $\alpha - \mu$ and exponential-generalized Gamma(EGG) distributions. The $\alpha - \mu$ distribution is a statistical model that is commonly used to describe the fading behavior of wireless channels, while the EGG distribution is a generalization of the Gamma distribution that can capture the effects of both fading and shadowing. By using these two distributions to model the DF relay in a hybrid RF-UOWC system, the authors were able to evaluate the system's confidentiality and assess its effectiveness in different scenarios. The authors of the paper are discussing the need for a unified statistical framework that can account for turbulence-induced attenuation in UOWC channels. The authors also mention the importance of studying the system's performance in Nakagami-m fading situations as discussed in another study referenced in [31].

The term "turbulence-induced attenuation" refers to the loss of signal strength that occurs due to the movement of water particles in the channel, which can cause fluctuations in the refractive index of the medium. However, a statistical framework that accounts for this attenuation would help in predicting the performance of the system in such channels and optimizing its design accordingly. The author's references to the above discussion and using a combined approach of Nakagami-m fading for a MIMO-RF and UOWC situations refer to a statistical model used to describe the fading behavior of wireless channels, which can be used to predict the probability of errors in the transmission of data. By studying the system's performance in such situations, the authors can gain insights into the factors

that affect the system's reliability and optimize its design accordingly.

C. CONTRIBUTIONS

This research's main contributions are a detailed examination of the MIMO RF-UOWC E2E system's efficacy, which is critical in improving the bandwidth performance of fifth-generation (5G) cellular networks. As a result, the following aspects of this study are stated.

- This work assumes that the transmitter side of the system is configured with the MIMO RF that utilizes the transmit antenna selection (TAS) technique. By merging the incoming signals using the maximum ratio combining (MRC) approach at the relay (R), which provides a source (S) for communicating with it. Upon combining with a UOWC link (D), it connects via R for establishing an overall secured link.
- In-depth analysis is done on the effectiveness of a hybrid MIMO RF-UOWC system, with the MIMO RF link simulated with the Nakagami-m channel and the UOWC hop modeled using the exponential and generalized Gamma (EGG) distributions, accordingly.
- An extensive study produces closed-form formulae for OP and BER in the framework of VGR for different means of detection utilizing heterodyne $r = 1$ and intensity modulation/direct detection (IM/DD) $r = 2$, respectively.
- Monte Carlo simulations are used to validate our statistical results to make sure they are accurate. The figures depict the findings for different bubble levels and various temperature variations at depths that have not yet been investigated in detail to date. Additionally, the findings of OP and BER are confirmed in terms of the average SNR of MIMO RF hop and electrical SNR of UOWC hop for a wide range of factors, including fading characteristics, number of antennae at receiver, bubble levels, temperature variations, and different modulation techniques.

To conclude, we tackle the combined dual-hop MIMO RF-UOWC system by developing accurate closed-form equations for the OP and BER of different binary modulation techniques. In continuation of previous work published in [32]; this work is an extension of a novel way of deriving a Cumulative Distribution Function (CDF) into a probability density function(pdf) along with new results involving different parameters as discussed earlier. As far as the authors are concerned, this system concept is still an open, unaddressed issue that requires more research based on the current literature.

D. ORGANISATION

The remainder of the work is organized as follows. The system and channels model are covered in Section II; the statistical characteristics of the E2E system are shown in Section III, whereas; the analytical OP and BER analyses are covered in Section IV, and the results of the numerical
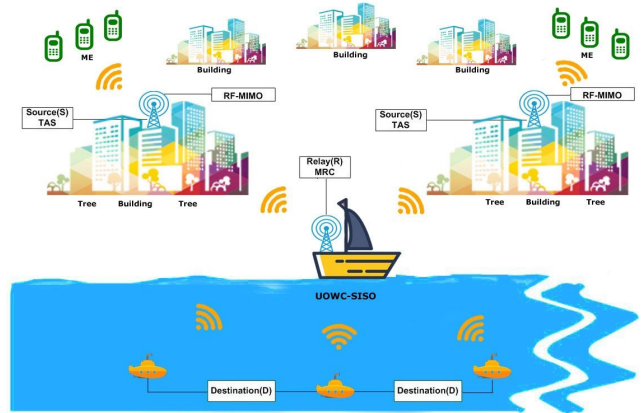

FIGURE 1. Hybrid MIMO RF-UOWC of a proposed system model. Transmitting antenna's N_T from the initial source node (S) to receiving antenna's N_R via relaying (R) node using VGR over an UOWC channel; the target node (D) gets the (R) node's message accordingly.

TABLE 1. EGG parameters based on expected and actual values for a UOWC system's temperature gradient.

BL	TG	(EGG) distribution
(L/min)	($°C\,cm^{-1}$)	(ω, λ, x, y, z)
(2.4)	(0.05)	(0.2131, 0.3292, 1.4298, 1.1818, 17.1985)
(2.4)	(0.10)	(0.2109, 0.2695, 0.6021, 1.2796, 21.1612)
(2.4)	(0.15)	(0.1808, 0.1642, 0.2335, 1.4202, 22.5925)
(2.4)	(0.20)	(0.1666, 0.1208, 0.1557, 1.5217, 22.8755)
(4.7)	(0.05)	(0.4588, 0.3448, 1.0423, 1.5767, 35.9425)
(4.7)	(0.10)	(0.4538, 0.2745, 0.3009, 1.7055, 54.1421)
(16.5)	(0.22)	(0.6235, 0.1095, 0.0112, 4.4751, 105.3552)
(23.6)	(0.22)	(0.7211, 0.1478, 0.0122, 7.4188, 65.6984)

simulations are discussed in Section V. Section VI gives some last remarks and suggestions in the conclusion and future work.

II. SYSTEM CONFIGURATION AND CHANNEL MODEL

A. SYSTEM CONFIGURATION

The system model is shown in Fig. 1, and the detailed explanation of the system includes clear illustrations of MIMO RF and UOWC hops. The system being examined implies that the array of antennas used for signal transmitting and receiving from S to R nodes is indicated by N_t and N_r, respectfully. MIMO RF channels are used for communication between the S and R nodes. The source node and destination node are connected through the relay node, and the relay node can communicate with both the source and destination nodes simultaneously because it is running in full-duplex mode. The communication from the relay node to the destination node is described as being a time-orthogonal transmission that happens sequentially in [32].

In the following step, the R node forwards along the indexing of the best transmitting and receiving antenna pairs, i.e., the channel with the highest absolute magnitude in [18]. When transmitting and receiving information that makes use of this information as feedback, a single antenna pair is chosen at random. Assuming the feedback is devoid of errors, defined as, where $|h_{xy}^{max}|$ is the sophistication of the channel,

TABLE 2. EGG parameters based on expected and actual values for Saline and Fresh water(Thermally Uniform) UOWC systems.

BL (L/min)	(EGG) distribution $(\omega, \lambda, x, y, z)$
Salty Water	
(2.4)	(0.1772, 0.4689, 0.7738, 1.1374, 49.1775)
(4.7)	(0.2066, 0.3955, 0.5309, 1.2156, 35.7366)
(7.1)	(0.4346, 0.4749, 0.3937, 1.4508, 77.0247)
(16.5)	(0.4953, 0.1369, 0.0163, 3.2035, 82.1032)
Fresh Water	
(2.4)	(0.1955, 0.5275, 3.7293, 1.0723, 30.3216)
(4.7)	(0.2107, 0.4605, 1.2528, 1.1503, 41.3256)
(7.1)	(0.3487, 0.4773, 0.4317, 1.4533, 74.3652)
(16.5)	(0.5119, 0.1604, 0.0077, 2.9965, 216.8358)

and the absolute magnitude value of the channel for the transmitter and receiver antennas we have chosen for the proposed system model.

$$|h_{\mathcal{XY}}^{max}| = \max_{i,j}\{|h_{\mathcal{XY}}^{i,j}|\}. \tag{1}$$

At MIMO RF, we illustrated the concept in [32] expressing the average energy and instantaneous SNRs of a channel.The following two tables from [32] have been used in this research to offer experimental knowledge of the parameters of the expectation maximization (EM) algorithm.

B. CHANNEL MODELS
Given the PDF illustrated in [33, eq. (11)], γ_{SR} of the MIMO-RF node, the expressed equation is presented below,

This PDF is affected by the total number of transmitting antennas, represented as N_T, the number of receiving antenna N_R, the Nakagami-m fading channel, and the instantaneous received SNR γ. The Gamma function [34, eq. (11.10)] is denoted as $\Gamma(.)$ and $\overline{\gamma}_{SR}$ is the average received SNR at the relay after the first hop.

The MRC technique is a receiver diversity technique used in wireless communication systems to combine the received signals from multiple antennas to improve the SNR and the quality of the signal. It involves multiplying each received signal by a weighting factor and adding the weighted signals together to produce a combined output signal. The weighting factors are chosen to maximize the SNR of the combined output signal. MRC can be used in both single-input single-output (SISO) and MIMO systems.The CDF of $\gamma_{SR} = max_{1 \leq i \leq N_T}\{\gamma_{SR,i}\}$ is obtained below,

$$f_{\gamma_{SR}}(\gamma) = \frac{N_T\, m^{N_R m}\, \gamma^{N_R m-1} e^{\frac{-m\gamma}{\overline{\gamma}_{SR}}}}{\Gamma(N_R m)\, \overline{\gamma}_{SR}^{N_R m}}$$

$$\times \left[1 - e^{\frac{-m\gamma}{\overline{\gamma}_{SR}}} \sum_{n=0}^{N_R m-1} \frac{1}{n!}\left(\frac{m\gamma}{\overline{\gamma}_{SR}}\right)^n\right]^{N_T-1}, \tag{2}$$

$$F_{\gamma_{SR}}(\gamma) = \left[1 - e^{\frac{-m\gamma}{\overline{\gamma}_{SR}}} \sum_{n=0}^{N_R m-1} \frac{1}{n!}\left(\frac{m}{\overline{\gamma}_{SR}}\gamma\right)^n\right]^{N_T}. \tag{3}$$

Using the power sum expansion and applying the binomial theorem, the following equations may be simplified from [35,

eq. (1.111)] and [36, eq. (9)], to acquire the expanded version of CDF for the MIMO-RF first hop,

$$F_{\gamma_{SR}}(\gamma) = \sum_{n=0}^{N_T}\binom{N_T}{n}(-1)^n e^{\frac{-n\gamma m}{\overline{\gamma}_{SR}}} \left\{\sum_{n_1=0}^{N_T}\sum_{n_2=0}^{n_1}\cdots\sum_{n_{N_R m-1}=0}^{n_{N_R m-2}}\right.$$

$$\left.\times\left[\prod_{k=1}^{N_R m-1}\binom{n_{k-1}}{n_k}\left(\frac{1}{k!}\right)^{n_k-n_{k+1}}\left(\frac{m}{\overline{\gamma}_{SR}}\right)^{n_k}\gamma^{n_k}\right]\right\}. \tag{4}$$

Here for simplicity $\zeta_1 = \sum_{n=0}^{N_T}\binom{N_T}{n}(-1)^n e^{\frac{-n\gamma m}{\overline{\gamma}_{SR}}}$, $\zeta_2 = \left\{\sum_{n_1=0}^{N_T}\sum_{n_2=0}^{n_1}\cdots\sum_{n_{N_R m-1}=0}^{n_{N_R m-2}}\right.$ and, $\zeta_3 = \left[\prod_{k=1}^{N_R m-1}\binom{n_{k-1}}{n_k}\right.$ $\left(\frac{1}{k!}\right)^{n_k-n_{k+1}}\left(\frac{m}{\overline{\gamma}_{SR}}\right)^{n_k}\gamma^{n_k}\left]\right\}$. According to [14], the exponential and generalised gamma distributions (EGG) are weighted together to form the EGG distribution, which is written as follows:

$$I = \omega_1 exp^{(\alpha_1,\beta_1)} + \omega_2 GG(\alpha_2,\beta_2,\gamma_2) \tag{5}$$

where ω_1 and ω_2 are the weights of the EGG, respectively, and $\alpha_1, \beta_1, \alpha_2, \beta_2$, and γ_2 are the shape parameters of the two distributions. The EGG distribution is useful for modeling the IF of optical waves because it can capture both the exponential and Gamma-like behavior of the fluctuations. This is important because the IF of an optical wave can be affected by different physical phenomena, such as air bubbles or temperature variations, which can have different statistical characteristics. By using the EGG distribution, it is possible to account for these different behaviors in a single mode

$$f_I(I) = \omega f(I,\lambda) + (1-\omega) g(I;[x,y,z]),$$

$$f(I:\lambda) = \frac{1}{\lambda}e^{-\frac{I}{\lambda}},$$

$$g(I;[x,y,z]) = z\frac{I^{xz-1}}{y^{xz}}\frac{e^{-\frac{I}{y}^z}}{\Gamma(x)}, \tag{6}$$

It is an iterative algorithm that starts with initial estimates for the model parameters and then refines these estimates at each iteration by using the expectation (E) step and the maximization (M) step.

Based on the most recent parameter estimations, the method determines the anticipated value of the entire data log-likelihood in the E step. By maximizing the anticipated value of the entire data log-likelihood acquired in the E phase, the method updates the parameter estimations in the M step. These two steps are repeated until the estimates of the parameters converge, at which point the algorithm has found the MLEs of the parameters.

In the context of the UOWC links you mentioned, the EM algorithm is being used to find the MLEs for the parameters ω, λ, x, y, and z of the mixture model consisting of the exponential and generalized Gamma distributions. The parameters x, y, and z are the parameters of the generalised Gamma distribution. These parameters are estimated by the EM algorithm so that the mixture model fits the data

as closely as possible. According to two distinct detection kinds of the UOWC linkages, the combined PDF is stated as [14]. Here $\psi_1 = \frac{\omega}{r\,\gamma} G_{0,1}^{1,0} \left[\frac{1}{\lambda} \left(\frac{\gamma}{\mu_r} \right)^{\frac{1}{r}} \Big| \begin{array}{c} - \\ 1 \end{array} \right]$ and $\psi_2 = \frac{z(1-\omega)}{r\,\gamma\,\Gamma(x)} G_{0,1}^{1,0} \left[\frac{1}{y^z} \left(\frac{\gamma}{\mu_r} \right)^{\frac{z}{r}} \Big| \begin{array}{c} - \\ x \end{array} \right]$ are expressed in the below pdf as;

$$f_{\gamma_{RD}}(\gamma) = \psi_1 + \psi_1. \tag{7}$$

Subsequently, the CDF, $F_\gamma(\gamma) = \int_0^\gamma f_\gamma(\gamma)\,d\gamma$, is obtained as $\psi_3 = \omega\,G_{1,2}^{1,1} \left[\frac{1}{\lambda} \left(\frac{\gamma}{\mu_r} \right)^{\frac{1}{r}} \Big| \begin{array}{c} 1 \\ 1,0 \end{array} \right]$ and $\psi_4 = \frac{(1-\omega)}{\Gamma(x)} G_{1,2}^{1,1} \left[\frac{1}{y^z} \left(\frac{\gamma}{\mu_r} \right)^{\frac{z}{r}} \Big| \begin{array}{c} 1 \\ x,0 \end{array} \right]$ expressed below,

$$F_{\gamma_{RD}}(\gamma)\,\psi_3 + \psi_4. \tag{8}$$

where in the case of heterodyne detection technique, the electrical SNR, μ_1, is defined as $\mu_1 = \overline{\gamma}_{RD}$, while for IM/DD technique, the electrical SNR, μ_2, is expressed as [14, eq. (19)]

III. STATISTICAL CHARACTERISTICS OF THE PROPOSED SYSTEM

The proposed statistical characteristics are presented using the VGR equation in [33] as,

$$F_{\gamma_{eq}} = \frac{\gamma_{SR}\,\gamma_{RD}}{\gamma_{SR} + \gamma_{RD} + 1}, \tag{9}$$

where γ_{SR} and γ_{RD} are the instantaneous SNR's for S-to-R and R-to-D nodes, respectively. In [1], it provides a precise estimate of the E2E SNR for VGR as;

$$F_{\gamma_{eq}} \approx min(\gamma_{SR}, \gamma_{RD}). \tag{10}$$

The CDF and pdf of the proposed system as shown in (11)–(13), as shown at the bottom of the next page, are obtained through extensive mathematical simplifications of the equations and utilizing the Wolfram Mathematica 12.1 respectively.

IV. PERFORMANCE ANALYSIS

A. OUTAGE PROBABILITY (OP)

Here in this section, we discuss the outage probability (OP) for the proposed E2E system. The Outage Probability (OP) is the probability that the combined MIMO-RF and UOWC system fails to meet a specific quality-of-service (QoS) requirement. Specifically, we calculate the probability that either the MIMO-RF or UOWC link experiences an outage.

Let's denote the OP for the MIMO-RF system as $OP_{MIMO-RF}$ and the OP for the UOWC system as OP_{UOWC}. The combined system's overall OP, denoted as $OP_{combined}$, is the probability of experiencing an outage in either the $MIMO-RF$ or $UOWC$ link, i.e., it is the union of $OP_{MIMO-RF}$ and OP_{UOWC}. Here both MIMO-RF and UOWC channels experience independent and identically distributed (i.i.d.) fading, following Nakagami-m distribution. The communication links are subject to additive white Gaussian noise (AWGN)

in both the RF and UOWC channels. The transmitter knows the channel state information (CSI) for spatial processing in MIMO-RF, and both the transmitter and receiver have knowledge of the channel characteristics in UOWC. On the contrary the accuracy of the OP calculation relies on the validity of the fading models and the availability of accurate channel information. The dynamic nature of the underwater environment and the RF channel can lead to variations in the communication link's performance, affecting the accuracy of the OP estimation.

The likelihood that the SNR drops below a certain threshold, γ_{th}, known as the outage probability (OP). In other words, it is the probability that the system fails to transmit data successfully due to poor signal quality. Therefore, P_{out} is given as [18, eq. (5)]

$$P_{out} = P_r\left[\gamma_{eq} < \gamma_{th} \right] = F_{\gamma_{eq}}(\gamma_{th}), \tag{14}$$

The overall $OP_{combined}$ represents the probability that either the MIMO-RF or the UOWC link experiences an outage. It gives an insight into the system's reliability in challenging environments where both RF and underwater optical communication are combined. By analyzing the $OP_{combined}$, system designers can assess the combined MIMO-RF and UOWC system's performance and make decisions regarding the necessary improvements or adjustments to achieve reliable and robust communication in 5G and beyond networks.

In conclusion, the outage probability calculation in MIMO-RF and UOWC systems requires a deep understanding of the channel characteristics and statistical properties. While OP is a valuable metric for assessing system reliability, it's essential to consider the assumptions and limitations when applying these calculations in real-world scenarios, especially in challenging environments like underwater communications.

B. AVERAGE BIT ERROR RATE (ABER)

In this section we understand the average bit error rate (ABER) calculation, we need to clarify the modulation parameters p and q. These parameters are used to represent the modulation schemes employed in the MIMO-RF and UOWC systems.

As a proportion of the total number of bits transferred, BER measures the number of inaccurately received bits in a transmission. BER is an essential parameter for assessing the effectiveness of a wireless communication system. Better performance is indicated by a lower BER since fewer transmission errors are currently made. This allows us study the effects of these characteristics on the effectiveness of the communication system. The probability of error rate is expressed as [37, eq. (12)]

$$P_e = \frac{q^p}{2\,\Gamma(p)} \int_0^\infty e^{-q\gamma}\,\gamma^{p-1}\,F_{\gamma_{eq}}(\gamma)\,d\gamma, \tag{15}$$

wherein the modulating parameters are p and q and are taken into consideration in continuation of our previous work published in [32]. In MIMO-RF systems, the parameter

p represents the modulation order used at the transmitter for each transmit antenna. It can be any positive integer, commonly taking values such as p = 2 for Binary Phase Shift Keying (BPSK), p = 4 for Quadrature Phase Shift Keying (QPSK), p = 16 for 16-QAM, etc. On the other side, in UOWC systems, the parameter q represents the modulation order used at the transmitter for the optical signals. Similar to p, q can also be any positive integer, representing the number of symbols used to encode information in each optical signal, such as q = 2 for On-Off Keying (OOK), q = 4 for Quadrature Amplitude Modulation (QAM), etc.

Here in our case we have used BER modulation type as Coherent Binary Frequency Shift Keying (CBFSK), Coherent Binary Phase Shift Keying (CBPSK), Non-Coherent Binary Frequency Shift Keying (NBFSK) and Differential Binary Phase Shift Keying (DBPSK) with varying p and q as explained in the table.

The average bit error rate(ABER) calculation provides insights into the overall performance of the proposed MIMO-RF and UOWC systems. The ABER for MIMO-RF reflects

TABLE 3. BER parameters of binary modulations.

BER Modulation Type (bits / sec)	p	q
Coherent Binary Frequency Shift Keying (CBFSK)	0.5	0.5
Coherent Binary Phase Shift Keying (CBPSK)	0.5	1
Non-Coherent Binary Frequency Shift Keying (NBFSK)	1	0.5
Differential Binary Phase Shift Keying (DBPSK)	1	1

how well the RF part of the system performs in terms of error probability based on the SNR. A lower ABER indicates better error resilience and higher data transmission accuracy. Similarly, the ABER for UOWC represents the error probability of the optical communication link based on the received optical power. A lower ABER implies that the UOWC part of the system can reliably transmit data with fewer errors.

The combined MIMO-RF and UOWC system's overall performance depends on both the MIMO-RF and UOWC components' individual BERs. A low BER for MIMO-RF indicates robust RF communication with minimal data errors,

$$F_{\gamma_{eq}}(\gamma) = \zeta_1\zeta_2\zeta_3 + \omega\, G_{1,2}^{1,1}\left[\frac{1}{\lambda}\left(\frac{\gamma}{\mu_r}\right)^{\frac{1}{r}} \Bigg|\begin{matrix}1\\1,0\end{matrix}\right] + \frac{(1-\omega)}{\Gamma(x)}G_{1,2}^{1,1}\left[\frac{1}{y^z}\left(\frac{\gamma}{\mu_r}\right)^{\frac{c}{r}}\Bigg|\begin{matrix}1\\x,0\end{matrix}\right]$$

$$\times -\zeta_1\zeta_2\zeta_3\omega\, G_{1,2}^{1,1}\left[\left(\frac{1}{\lambda}\right)\left(\frac{\gamma}{\mu_r}\right)^{\frac{1}{r}}\Bigg|\begin{matrix}1\\1,0\end{matrix}\right] - \zeta_1\zeta_2\zeta_3\frac{(1-\omega)}{\Gamma(x)}G_{1,2}^{1,1}\left[\frac{1}{y^z}\left(\frac{\gamma}{\mu_r}\right)^{\frac{z}{r}}\Bigg|\begin{matrix}1\\x,0\end{matrix}\right] \tag{11}$$

$$F_{\gamma_{eq}}(\gamma) = \zeta_1\zeta_2\zeta_3 + \psi_3 + \psi_4 - \zeta_1\zeta_2\zeta_3\psi_3 - \zeta_1\zeta_2\zeta_3\psi_4 \tag{12}$$

$$f_{\gamma_{eq}}(\gamma) = \frac{\omega\left(\frac{\gamma}{\mu_r}\right)^{-1+\frac{1}{r}}}{r\lambda\mu_r} + \frac{e^{-\frac{\left(\frac{\gamma}{\mu_r}\right)^{\frac{1}{r}}}{\lambda}}\left(1-e^{\frac{\left(\frac{\gamma}{\mu_r}\right)^{\frac{1}{r}}}{\lambda}}\right)\omega\left(\frac{\gamma}{\mu_r}\right)^{-1+\frac{1}{r}}}{r\lambda\mu_r}$$

$$+ \frac{y^{-z}ze^{-y^{-z}\left(\frac{\gamma}{\mu_r}\right)^{z/r}}(1-\omega)\left(y^{-z}\left(\frac{\gamma}{\mu_r}\right)^{z/r}\right)^{-1+x}\left(\frac{\gamma}{\mu_r}\right)^{-1+\frac{z}{r}}\mathrm{Gamma}[x]}{r\Gamma\mu_r\mathrm{Gamma}[1+x]}$$

$$- \frac{\zeta_1\omega\left(\frac{\gamma}{\mu_r}\right)^{-1+\frac{1}{r}}\left\{e^{-\frac{n\gamma m}{\overline{\gamma}_{SR}}}\right\}[\zeta_2\zeta_3\gamma^{n_k}]}{r\lambda\mu_r} - \frac{\zeta_1 e^{-\frac{\left(\frac{\gamma}{\mu_r}\right)^{\frac{1}{r}}}{\lambda}}\left(1-e^{\frac{\left(\frac{\gamma}{\mu_r}\right)^{\frac{1}{r}}}{\lambda}}\right)\omega\left(\frac{\gamma}{\mu_r}\right)^{-1+\frac{1}{r}}\left\{e^{-\frac{n\gamma m}{\overline{\gamma}_{SR}}}\right\}[\zeta_2\zeta_3\gamma^{n_k}]}{r\lambda\mu_r}$$

$$- \frac{\zeta_1 y^{-z}ze^{-y^{-z}\left(\frac{\gamma}{\mu_r}\right)^{z/r}}(1-\omega)\left(y^{-z}\left(\frac{\gamma}{\mu_r}\right)^{z/r}\right)^{-1+a}\left(\frac{\gamma}{\mu_r}\right)^{-1+\frac{z}{r}}\mathrm{Gamma}[x]\left\{e^{-\frac{n\gamma m}{\overline{\gamma}_{SR}}}\right\}[\zeta_2\zeta_3\gamma^{n_k}]}{r\Gamma\mu_r\mathrm{Gamma}[1+x]}$$

$$+ \zeta_1\left(\{0\}\left[\zeta_2\zeta_3\gamma^{n_k}\right] + \zeta_2\zeta_3 n_k\gamma^{-1+n_k}\left\{e^{-\frac{n\gamma m}{\overline{\gamma}_{SR}}}\right\}'\left[\zeta_2\zeta_3\gamma^{n_k}\right]\right)$$

$$+ \zeta_1 e^{-\frac{\left(\frac{\gamma}{\mu_r}\right)^{\frac{1}{r}}}{\lambda}}\left(1-e^{\frac{\left(\frac{\gamma}{\mu_r}\right)^{\frac{1}{r}}}{\lambda}}\right)\omega\left(\{0\}\left[\zeta_2\zeta_3\gamma^{n_k}\right] + \zeta_2\zeta_3 n_k\gamma^{-1+n_k}\left\{e^{-\frac{n\gamma m}{\overline{\gamma}_{SR}}}\right\}'\left[\zeta_2\zeta_3\gamma^{n_k}\right]\right)$$

$$- \frac{\zeta_1(1-\omega)\mathrm{Gamma}[x]\mathrm{Gamma}\left[x,0,y^{-z}\left(\frac{\gamma}{\mu_r}\right)^{z/r}\right]\left(\{0\}\left[\zeta_2\zeta_3\gamma^{n_k}\right] + \zeta_2\zeta_3 n_k\gamma^{-1+n_k}\left\{e^{-\frac{n\gamma m}{\overline{\gamma}_{SR}}}\right\}'\left[\zeta_2\zeta_3\gamma^{n_k}\right]\right)}{\Gamma\mathrm{Gamma}[1+x]} \tag{13}$$
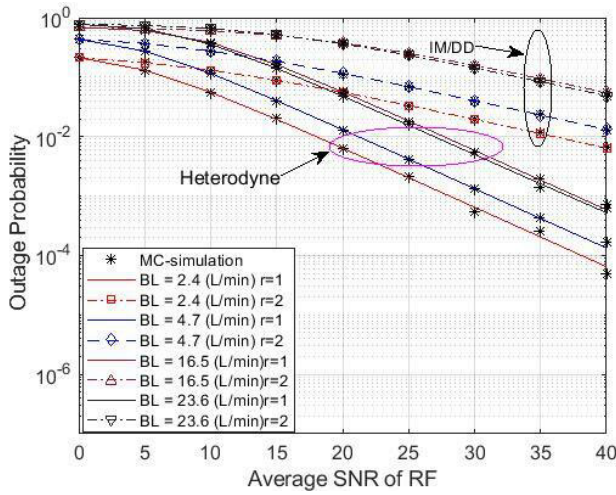
FIGURE 2. OP vs.(S-R) RF average SNR for different BL's under different modes of detection via R-D UOWC.
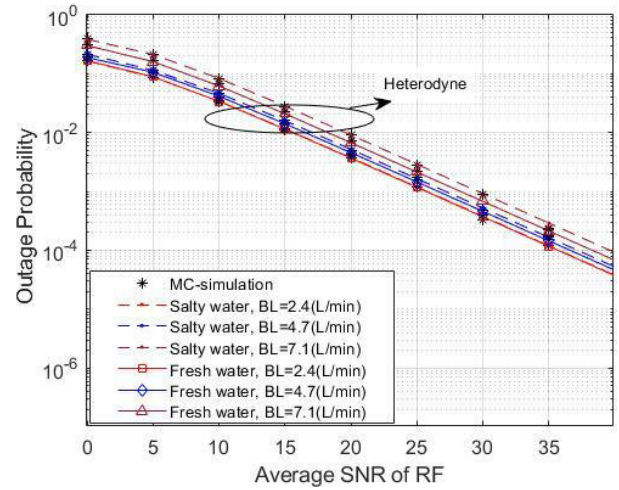

FIGURE 4. OP vs.(S-R) RF average SNR for different BL's under different (Fresh/Salty) waters via R-D UOWC.
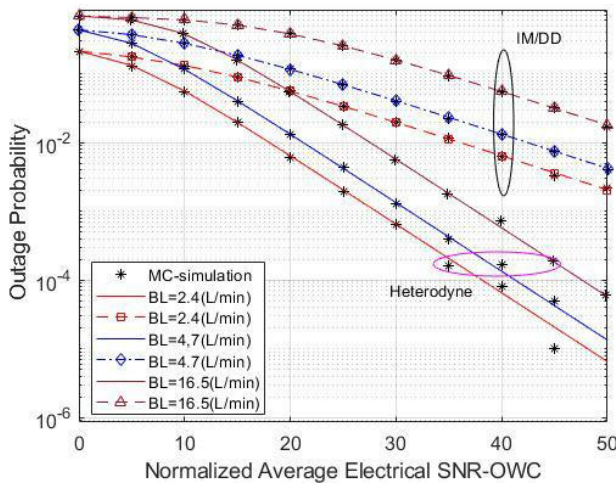

FIGURE 3. OP vs. (R-D) UOWC electrical SNR for different BL's under different modes of detection via R-D UOWC.
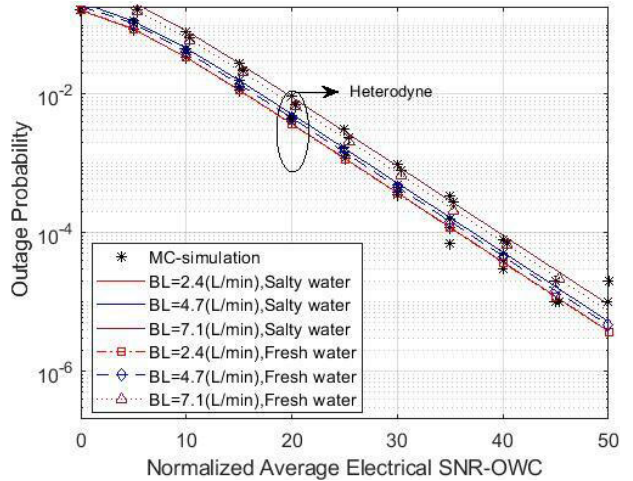

FIGURE 5. OP vs. (R-D) UOWC electrical SNR for different BL's under different (Fresh/Salty) waters via R-D UOWC.

while a low BER for UOWC indicates reliable underwater optical communication. By considering both BERs, the overall system's performance can be analyzed under various scenarios, accounting for the different environmental conditions and challenges in both RF and underwater optical communication. The proposed system's success lies in achieving acceptable BERs for both MIMO-RF and UOWC, thus ensuring reliable and accurate data transmission in 5G and beyond networks, particularly in complex and dynamic environments.

In order to obtain the average BER for our proposed E2E system, we thus put (11) into (15) and solving the complex analysis to derive the desired probability of error.

Subsequently, employing and implementing the probability of error for P_{e_a}, P_{e_b}, P_{e_c}, P_{e_d}, and P_{e_e} respectively in parts, our derived probability of error is illustrated in the figures given in the results section.

V. RESULTS OBTAINED FROM ANALYTICAL-BASED SIMULATIONS

The outcomes of Monte-Carlo (MC) simulations assessing the applicability of OP and BER to our proposed E2E system are discussed in this section. Then the testing and validation of a wireless communication system that uses both RF and UOWC channels are analyzed in a dual-hop system. The system's performance is evaluated using MC simulations, which consider the effects of different factors such as temperature gradients, modulation techniques, and fading conditions with variable numbers of antennas. The total number of antennas is fixed at Nt = Nr = 4 in the first hop, and the parameter r expresses two different types of detecting techniques. The behavior of signals in UOWC alters with an increase in the bubble levels (BL), which causes fluctuations in Fig. 2 and 3 due to the phenomenon of refractive index. The results show that raising the BL from
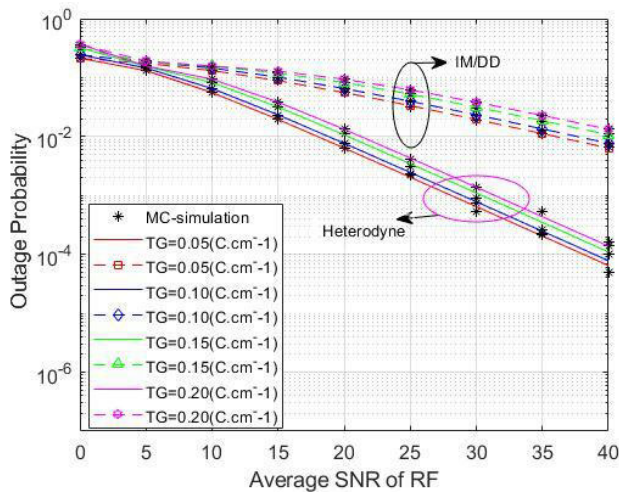
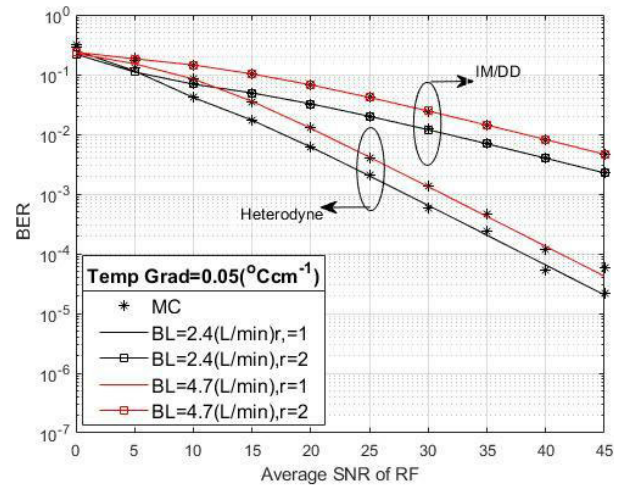**FIGURE 6.** OP vs. (S-R) RF average SNR for different TG's under different modes of detection via R-D UOWC.

FIGURE 8. BER vs. (S-R) RF average SNR for different BL's under different modes of detection via R-D UOWC.
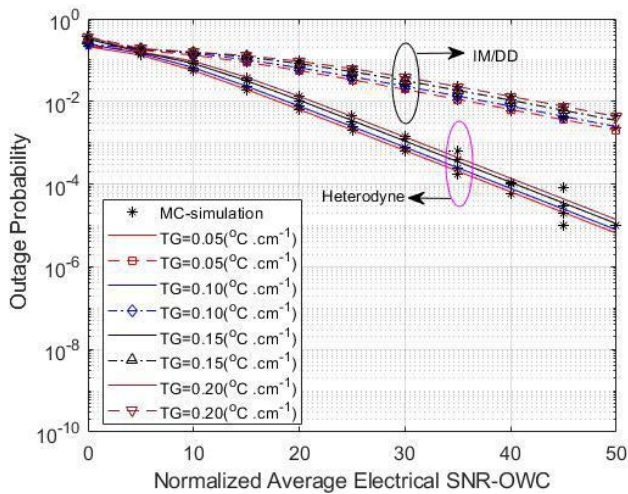

FIGURE 7. OP vs.(R-D) UOWC electrical SNR for different TG's under different modes of detection via R-D UOWC.
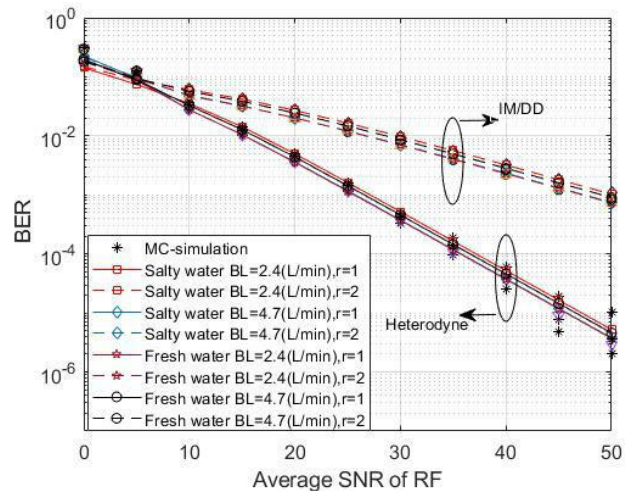

FIGURE 9. BER vs. (S-R) RF average SNR for different BL under different (Fresh/Salty)waters via R-D UOWC.

2.4 (L/min) to 23.6 (L/min) results in a higher OP at the targeted average SNR. The heterodyne approach achieves superior performance to intensity modulation/direct detection (IM/DD) technology, as demonstrated by the fact that OP with r = 1 surpasses that with r = 2. These fluctuations are caused by changes in air bubbles, temperature, and salty and fresh water, which create fading in signal and reduce the effectiveness of the UOWC system.

Figs. 4 and 5 exhibit the BLs' varying behavior in both fresh as well as saline water while maintaining the other values as listed in Table. 2. The MC simulations and the analytical findings agree exactly, supporting the validity of the obtained analysis.

In summary, the text explains how the system's performance is evaluated using Monte Carlo simulations, which consider the effects of different factors such as temperature

gradients, modulation techniques, and fading conditions with variable numbers of antennas.

The effect of temperature on the performance of the heterodyne detection technique in the UOWC system is discussed, with the technique performing better at a temperature of $0.05 \, (^{\circ}C \, cm^{-1})$ compared to higher temperatures of maximum temperature computed in our proposed case of $0.20 \, (^{\circ}C \, cm^{-1})$, indicating that the performance of the system changes with temperature as seen in Figs. 6 and 7 for different detection methods in the UOWC channel.

Temperature affects turbulence in the UOWC system, which in turn affects its outage probability and reliability, highlighting the need to consider temperature in ensuring reliable communication.

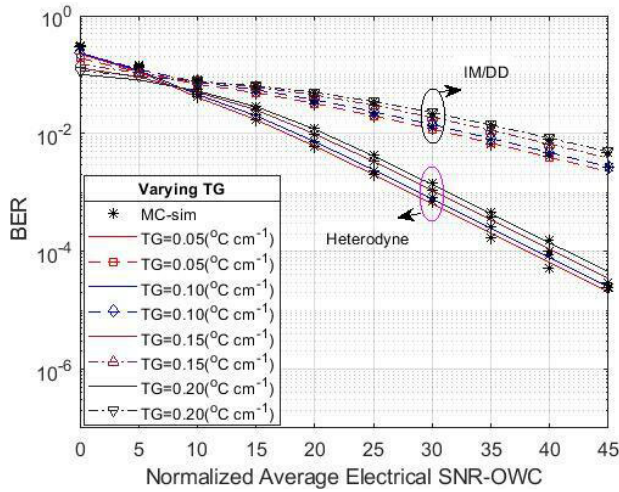In Fig. 8, BER results for several BLs pertinent to the studied E2E system are shown versus the average SNR of RF

FIGURE 10. BER vs. (R-D) UOWC electrical SNR for different TG's under different mode of detection via R-D UOWC.
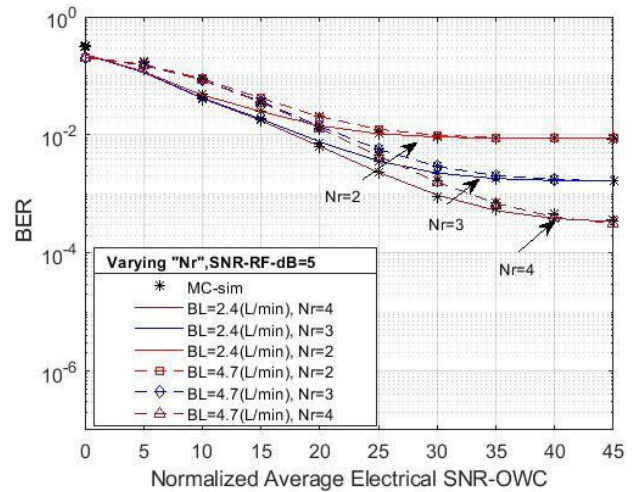

FIGURE 12. BER vs. (R-D) UOWC electrical SNR for different Received Antenna's N_r under different BL's via R-D UOWC.
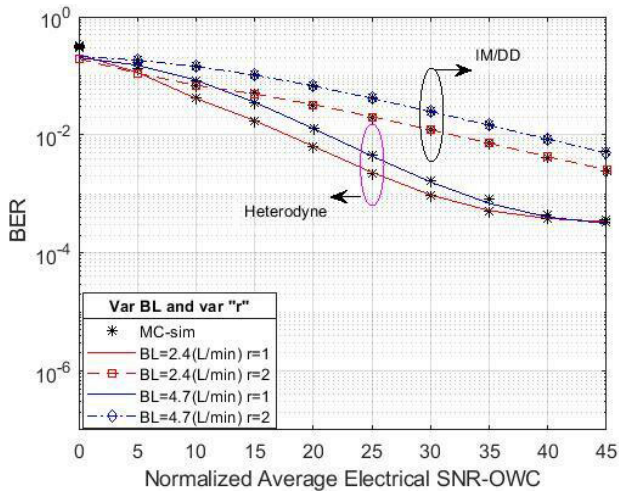

FIGURE 11. BER vs. (R-D) UOWC electrical SNR for different BL under different mode of detection via R-D UOWC.
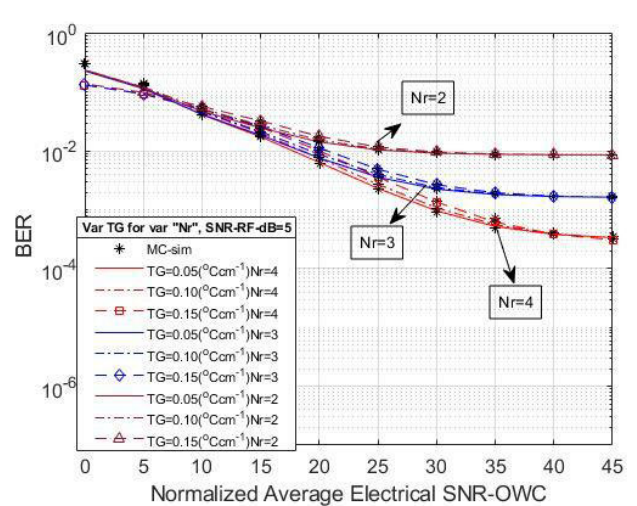

FIGURE 13. BER vs. (R-D) UOWC electrical SNR for different Received Antenna's N_r under different TG's via R-D UOWC.

hop. For a range of BLs between 2.4 and 4.7 L/min, we saw a favorable response.

The behavior of saltiness affects signal levels in UOWC and fresh water with BL = $2.4(L/min)$ which outperforms the saline water as shown in Fig. 9.

The performance of BER in the UOWC link is critical and depends on the varied ranges of BL under different circumstances. The plots in Figs. 10, 11, 12, and 13 show the BER vs SNR for UOWC hop with varied $TG's$ and $BL's$, and altering number of antennae for the receiving end N_R at the initial hop. Adding more antennae at the S-R hop for studying the performance of our proposed wireless communication system.

According to the study, raising the number of antennas, increased system efficiency in real-time circumstances, as shown by the figures presented in the form of BLs and TGs. However, increasing the electrical SNR (signal-to-noise ratio)

did not improve performance due to the average SNR of the RF hop acting as a restriction. This means that the number of increased antennas is a more effective way to improve the system's performance than increasing the electrical SNR. The study provides insight into how the system performs under different environmental conditions and can help optimize the system for better performance.

In Fig. 14 to Fig.15, the BER plots are generated against the electrical and average SNR's for different BL's and TG's values.

The results provide insight into how the system performs under different environmental conditions and can help optimize the system for better performance. Finally, binary modulation methods are used to convert digital data into a binary format that can be transmitted over a channel for more reliable and secured data communication.
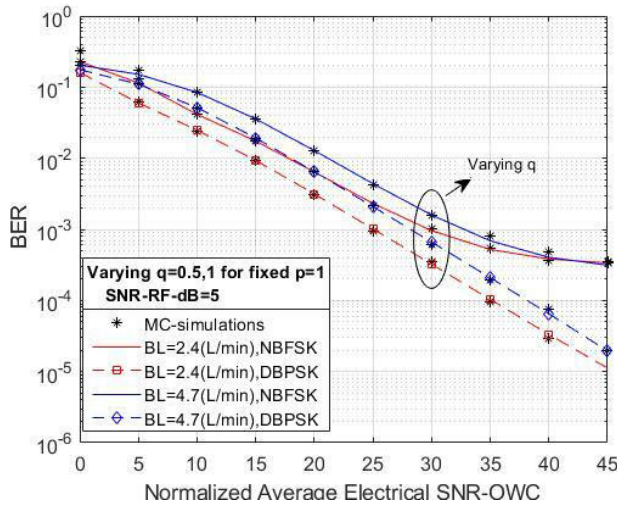
FIGURE 14. BER vs. (R-D) UOWC electrical SNR for different modulation schemes under different BL's via R-D UOWC.
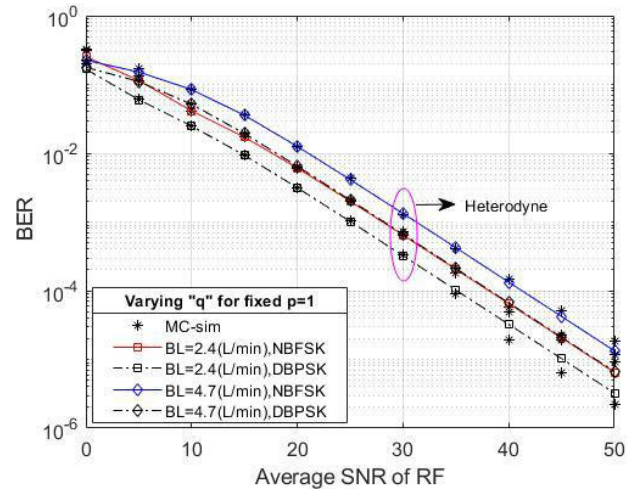

FIGURE 16. BER vs. (S-R) RF average SNR for different modulation scheme's under different BL's via R-D UOWC.
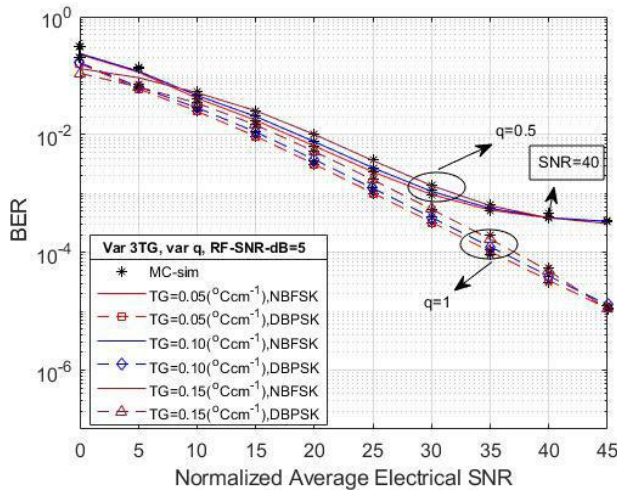

FIGURE 15. BER vs. (R-D) UOWC electrical SNR for different modulation schemes under different TG's via R-D UOWC.
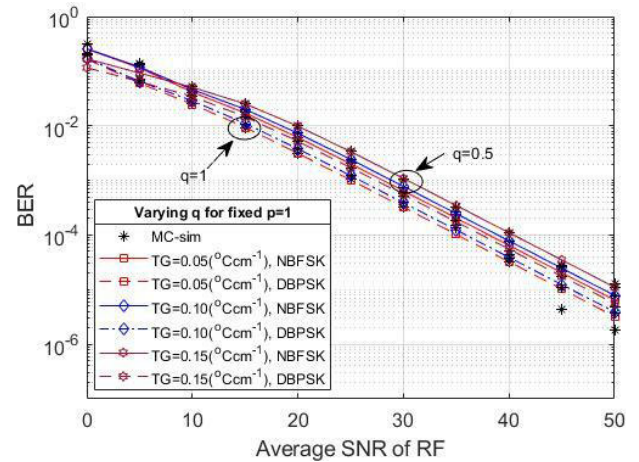

FIGURE 17. BER vs. (S-R) RF average SNR for different modulation scheme's under different TG's via R-D UOWC.

In DBPSK, phase modulation changes the phase of the carrier signal to represent the binary data. In this method, the phase of the carrier signal is shifted by 180 degrees if the binary data is a 1, and remains unchanged if the binary data is a 0. This modulation method is called "differential" because the phase shift is relative to the previous bit, rather than an absolute phase shift. While in NBFSK, on the other hand, a frequency modulation changes the frequency of the carrier signal to represent the binary data. In this method, two different frequencies are used to represent the two binary values.

The frequency of the carrier signal is shifted to a higher frequency if the binary data is a 1, and to a lower frequency if the binary data is a 0. This modulation method is called "non-coherent" because it does not require the receiver to know the carrier frequency. Both DBPSK and NBFSK are binary modulation methods, meaning they are used to transmit

binary data (0s and 1s) over a communication channel. These methods are used in the wireless communication system discussed in the paper to improve communication performance under different system and channel characteristics.

The DBPSK modulation method performs better than NBFSK in the proposed dual-hop communication system due to the average RF hop SNR acting as a restriction, causing a corresponding floor within the NBFSK curve at the UOWC electrical SNRs that we noticed due to this experimentation work.

VI. CONCLUSION AND FUTURE WORK

This paper concluded on the derivation of the closed-form formulae for the outage probability (OP) and average bit error rate (BER) of our proposed dual-hop end-to-end (E2E) communication system, via utilizing Meijer's G function. The study provided valuable insights into system and channel parameters, including the effects of different detection

techniques in underwater-over-water communications with water turbulence, and it considered varying temperature and bubble levels along with multiple antennae at receiver end of relay station and the different modulation schemes in underwater.

The conclusions from this research are significant in several ways. Firstly, it presents a comprehensive analysis of the performance of the proposed dual-hop E2E system, offering crucial design guidelines for real-world implementation. Then the derived closed-form formulae provide a deeper understanding of system behavior, helping optimize communication links in challenging environments. Furthermore, this work lays the groundwork for future research directions; specifically, the investigation of ergodic capacity, multiple antenna techniques, cross-layer optimization, and real-world experiments for the proposed dual-hop E2E system can be extended by exploring various antenna combining techniques, ranging from conventional MIMO to more advanced Massive MIMO communication systems. These investigations could significantly enhance the system's capacity, leading to more efficient and robust communication in both underwater and over-water scenarios. By pursuing these research directions, we can unlock new insights into underwater-over-water communications and advance the field, leading to more robust, efficient, and reliable communication systems in challenging environments.

REFERENCES

[1] E. Illi, F. El Bouanani, D. B. D. Costa, F. Ayoub, and U. S. Dias, "Dual-hop mixed RF-UOW communication system: A PHY security analysis," *IEEE Access*, vol. 6, pp. 55345–55360, 2018.

[2] Z. Zeng, S. Fu, H. Zhang, Y. Dong, and J. Cheng, "A survey of underwater optical wireless communications," *IEEE Commun. Surveys Tuts.*, vol. 19, no. 1, pp. 204–238, 1st Quart., 2017.

[3] A. Celik, N. Saeed, B. Shihada, T. Y. Al-Naffouri, and M.-S. Alouini, "End-to-end performance analysis of underwater optical wireless relaying and routing techniques under location uncertainty," *IEEE Trans. Wireless Commun.*, vol. 19, no. 2, pp. 1167–1181, Feb. 2020.

[4] M. Elamassie, F. Miramirkhani, and M. Uysal, "Performance characterization of underwater visible light communication," *IEEE Trans. Commun.*, vol. 67, no. 1, pp. 543–552, Jan. 2019.

[5] M. Elamassie and M. Uysal, "Vertical underwater visible light communication links: Channel modeling and performance analysis," *IEEE Trans. Wireless Commun.*, vol. 19, no. 10, pp. 6948–6959, Oct. 2020.

[6] M. V. Jamali, P. Khorramshahi, A. Tashakori, A. Chizari, S. Shahsavari, S. AbdollahRamezani, M. Fazelian, S. Bahrani, and J. A. Salehi, "Statistical distribution of intensity fluctuations for underwater wireless optical channels in the presence of air bubbles," in *Proc. Iran Workshop Commun. Inf. Theory (IWCIT)*, May 2016, pp. 1–6.

[7] M. V. Jamali, A. Mirani, A. Parsay, B. Abolhassani, P. Nabavi, A. Chizari, P. Khorramshahi, S. Abdollahramezani, and J. Salehi, "Statistical studies of fading in underwater wireless optical channels in the presence of air bubble, temperature, and salinity random variations (long version)," *IEEE Trans. Commun.*, vol. 66, no. 10, pp. 4706–4723, Oct. 2018.

[8] E. Zedini, H. M. Oubei, A. Kammoun, M. Hamdi, B. S. Ooi, and M.-S. Alouini, "A new simple model for underwater wireless optical channels in the presence of air bubbles," in *Proc. GLOBECOM IEEE Global Commun. Conf.*, Dec. 2017, pp. 1–6.

[9] B. M. Cochenour, "Experimental measurements of temporal dispersion for underwater laser communications and imaging," North Carolina State Univ., Raleigh, NC, USA, Tech. Rep. 8304, 2013.

[10] B. Cochenour, L. Mullen, A. Laux, and E. P. Zege, "Spatial and temporal effects of forward scattering on an intensity modulated source for laser communications underwater," Dept. Elect. Eng., North Carolina State Univ., Raleigh, NC, USA, Tech. Rep. OO080430, 2008.

[11] B. Cochenour, A. Laux, and L. Mullen, "Temporal dispersion in underwater laser communication links: Closing the loop between model and experiment," in *Proc. IEEE 3rd Underwater Commun. Netw. Conf. (UComms)*, Aug. 2016, pp. 1–5.

[12] W. Cox and J. Muth, "Simulating channel losses in an underwater optical communication system," *J. Opt. Soc. Amer. A, Opt. Image Sci.*, vol. 31, no. 5, p. 920, May 2014.

[13] C. ben Issaid and M.-S. Alouini, "Efficient estimation of the left tail of bimodal distributions with applications to underwater optical communication systems," 2019, *arXiv:1909.11016*.

[14] E. Zedini, H. M. Oubei, A. Kammoun, M. Hamdi, B. S. Ooi, and M.-S. Alouini, "Unified statistical channel model for turbulence-induced fading in underwater wireless optical communication systems," *IEEE Trans. Commun.*, vol. 67, no. 4, pp. 2893–2907, Apr. 2019.

[15] S. Kumar, S. Prince, J. V. Aravind, and G. S. Kumar, "Analysis on the effect of salinity in underwater wireless optical communication," *Mar. Georesources Geotechnol.*, vol. 38, no. 3, pp. 291–301, Mar. 2020.

[16] E. Zedini, A. Kammoun, H. Soury, M. Hamdi, and M.-S. Alouini, "Performance analysis of dual-hop underwater wireless optical communication systems over mixture exponential-generalized gamma turbulence channels," *IEEE Trans. Commun.*, vol. 68, no. 9, pp. 5718–5731, Sep. 2020.

[17] Z. Chen, Z. Chi, Y. Li, and B. Vucetic, "Error performance of maximal-ratio combining with transmit antenna selection in flat Nakagami-*m* fading channels," *IEEE Trans. Wireless Commun.*, vol. 8, no. 1, pp. 424–431, Jan. 2009.

[18] N. Yang, M. Elkashlan, and J. Yuan, "Dual-hop amplify-and-forward MIMO relaying with antenna selection in Nakagami-*m* fading," in *Proc. IEEE Global Telecommun. Conf. (GLOBECOM)*, Dec. 2010, pp. 1–6.

[19] P. L. Yeoh, M. Elkashlan, and I. B. Collings, "MIMO relaying: Distributed TAS/MRC in Nakagami-*m* fading," *IEEE Trans. Commun.*, vol. 59, no. 10, pp. 2678–2682, Oct. 2011.

[20] T. Gucluoglu and T. M. Duman, "Performance analysis of transmit and receive antenna selection over flat fading channels," *IEEE Trans. Wireless Commun.*, vol. 7, no. 8, pp. 3056–3065, Aug. 2008.

[21] Z. Vali, A. Gholami, Z. Ghassemlooy, M. Omoomi, and D. G. Michelson, "Experimental study of the turbulence effect on underwater optical wireless communications," *Appl. Opt.*, vol. 57, no. 28, p. 8314, Oct. 2018.

[22] Y. Lou, R. Sun, J. Cheng, G. Qiao, and J. Wang, "Physical-layer security for UAV-assisted air-to-underwater communication systems with fixed-gain amplify-and-forward relaying," *Drones*, vol. 6, no. 11, p. 341, Nov. 2022.

[23] F. D. Ledezma, A. Amer, F. Abdellatif, A. Outa, H. Trigui, S. Patel, and R. Binyahib, "A market survey of offshore underwater robotic inspection technologies for the oil and gas industry," in *Proc. SPE Saudi Arabia Sect. Annu. Tech. Symp. Exhib.*, 2015, pp. 1–7.

[24] H. Kaushal and G. Kaddoum, "Underwater optical wireless communication," *IEEE Access*, vol. 4, pp. 1518–1547, 2016.

[25] B. Pranitha and L. Anjaneyulu, "Analysis of underwater acoustic communication system using equalization technique for ISI reduction," *Proc. Comput. Sci.*, vol. 167, pp. 1128–1138, Jan. 2020.

[26] A. C. Boucouvalas, K. P. Peppas, K. Yiannopoulos, and Z. Ghassemlooy, "Underwater optical wireless communications with optical amplification and spatial diversity," *IEEE Photon. Technol. Lett.*, vol. 28, no. 22, pp. 2613–2616, Nov. 15, 2016.

[27] I. Zakaria, M. Abaza, M. Fedawy, and M. H. Aly, "Performance analysis of hybrid free space optical and visible light communications for underwater applications using spatial diversity," *Opt. Quantum Electron.*, vol. 54, no. 10, p. 650, Oct. 2022.

[28] A. Samir, M. Elsayed, A. A. A. El-Banna, I. S. Ansari, K. Rabie, and B. M. ElHalawany, "Performance analysis of dual-hop hybrid RF-UOWC NOMA systems," *Sensors*, vol. 22, no. 12, p. 4521, Jun. 2022.

[29] H. M. Oubei, E. Zedini, R. T. ElAfandy, A. Kammoun, M. Abdallah, T. K. Ng, M. Hamdi, M.-S. Alouini, and B. S. Ooi, "Simple statistical channel model for weak temperature-induced turbulence in underwater wireless optical communication systems," *Opt. Lett.*, vol. 42, no. 13, p. 2455, 2017.

[30] Y. Lou, R. Sun, J. Cheng, D. Nie, and G. Qiao, "Secrecy outage analysis of two-hop decode-and-forward mixed RF/UWOC systems," *IEEE Commun. Lett.*, vol. 26, no. 5, pp. 989–993, May 2022.

[31] H. Lei, Y. Zhang, K.-H. Park, I. S. Ansari, G. Pan, and M.-S. Alouini, "Performance analysis of dual-hop RF-UWOC systems," *IEEE Photon. J.*, vol. 12, no. 2, pp. 1–15, Apr. 2020.

[32] I. S. Ansari, L. Jan, Y. Tang, L. Yang, and M. H. Zafar, "Outage and error analysis of dual-hop TAS/MRC MIMO RF-UOWC systems," *IEEE Trans. Veh. Technol.*, vol. 70, no. 10, pp. 10093–10104, Oct. 2021.

[33] N. Yang, P. L. Yeoh, M. Elkashlan, R. Schober, and I. B. Collings, "Transmit antenna selection for security enhancement in MIMO wiretap channels," *IEEE Trans. Commun.*, vol. 61, no. 1, pp. 144–154, Jan. 2013.

[34] M. H. Protter and B. Charles Jr., *A First Course in Real Analysis*, 2nd ed. New York, NY, USA: Springer, 1991, p. 536.

[35] D. Zwillinger and V. Moll, *Table of Integrals, Series, and Products*, 8th ed. New York, NY, USA: Academic, 2014, p. 17.

[36] S. Choi and Y.-C. Ko, "Performance of selection MIMO systems with generalized selection criterion over Nakagami-*m* fading channels," *IEICE Trans. Commun.*, vol. E89-B, no. 12, pp. 3467–3470, Dec. 2006.

[37] I. S. Ansari, S. Al-Ahmadi, F. Yilmaz, M.-S. Alouini, and H. Yanikomeroglu, "A new formula for the BER of binary modulations with dual-branch selection over generalized-K composite fading channels," *IEEE Trans. Commun.*, vol. 59, no. 10, pp. 2654–2658, Oct. 2011.

LATIF JAN (Member, IEEE) received the Ph.D. degree in electrical engineering with a specialization in wireless communication and networking from the University of Engineering and Technology (UET), Peshawar, Pakistan. Since 2022, he has been an Assistant Professor with Iqra National University (INU), Peshawar. His research interests include the field of optical wireless communication systems, physical layer security, free space optics for MIMO and massive MIMO technologies, and artificial intelligence using machine learning and deep learning.

GHASSAN HUSNAIN received the B.E. degree, the M.Sc. degree in network systems from the University of Sunderland, U.K., and the Ph.D. degree in intelligent ad hoc networks and bio-inspired computation from the University of Engineering and Technology, Peshawar, Pakistan. He is currently an Assistant Professor with Iqra National University, Peshawar. His research interests include intelligent systems, vehicular ad hoc networks, evolutionary computation, bio-inspired algorithms, and artificial intelligence.

WALEED TARIQ SETHI was born in Peshawar, Pakistan. He received the Ph.D. degree in telecommunication engineering from the University of Rennes 1, France, in 2018. He continued to build on his research while doing his Ph.D. as an Antenna Design Researcher with the KACST-Technology Innovation Center in RF and Photonics for the e-Society (RFTONICS), hosted at King Saud University, Saudi Arabia. He is currently an Assistant Professor with the Ghulam Ishaq Khan Institute of Engineering Sciences and Technology, Pakistan. He is tasked with teaching basic communication and electronic courses along with supervising projects of undergraduate and graduate students in the field of electromagnetism. His research topic was the novel design of optical antennas for harvesting solar radiation energy. During that span of two years, he published numerous ISI-indexed journals and was awarded three U.S. patents for proposing an omnidirectional indoor antenna for GSM and WLAN applications. His research interests include antenna designs in the microwave, millimeter wave and terahertz (THz) domain, wireless power transfer and ambient wireless energy harvesting, nanoantenna designs, and dielectric resonator antennas.

IHTISHAM UL HAQ received the bachelor's degree in mechatronics engineering and the master's degree in automation and control from the University of Engineering and Technology, Peshawar (UET Peshawar), in 2022, where he is currently pursuing the Ph.D. degree with the Mechatronics Department. He was a Research Assistant with NCAI, UET Peshawar, from June 2021 to June 2022, and as a Laboratory Engineer with the Mechatronics Department, UET Peshawar, for two years, from 2019 to 2021. He is a Research Associate with NCAI, UET Peshawar. His research interests include clinical image processing, artificial intelligence, machine learning, deep learning, and eXplainable AI.

YAZEED YASIN GHADI received the Ph.D. degree in electrical and computer engineering from Queensland University. He is currently an Assistant Professor of software engineering with Al Ain University. He was a Postdoctoral Researcher with Queensland University before joining Al Ain University. He has published more than 80 peer-reviewed journal articles and conference papers. He holds three pending patents. His current research interests include developing novel electro-acoustic-optic neural interfaces for large-scale high-resolution electrophysiology and distributed optogenetic stimulation. He was a recipient of several awards. He received the Sigma Xi Best Ph.D. Thesis Award for his dissertation on developing novel hybrid plasmonic photonic on-chip biochemical sensors.

HEND KHALID ALKAHTANI received the Bachelor of Science degree in computer science from the School of Engineering and Applied Science, The George Washington University in 1992, the Master of Science degree in information management from the Department of Engineering Management, George Washington University in 1993, and the Ph.D. degree in information security from the Department of Computer Science, Loughborough University in 2018. She is currently working as an Assistant Professor with the Princess Nourah Bint Abdulrahman University, College of Computer and Information Sciences Information Systems Department. She has 23 years of work experience as a Lecturer, worked as a computer center president, and as a statistic center president in faculty colleges. She is a member of the IEEE Society. She received an award from SIDF Academy: Leading Creative Transformation in Critical Time Program, Stanford University, Center for Professional Development.

● ● ●